Correlation of Full-Scale Isolated Proprotor Performance and Loads

Sesi Kottapalli
Aerospace Engineer
Aeromechanics Office, NASA Ames Research Center
Moffett Field, California, USA

C. W. Acree, Jr.
Ames Associate
Aeromechanics Office, NASA Ames Research Center
Moffett Field, California, USA

ABSTRACT

A full-scale isolated proprotor test was recently conducted in the USAF National Full-Scale Aerodynamics Complex (NFAC) at NASA Ames Research Center. The test article was a 3-bladed research rotor derived from the right-hand rotor of the AW609. For this test, the NASA Tiltrotor Test Rig (TTR) and rotor were installed in the 40- by 80-foot test section. This paper presents initial correlations between data and predictions of rotor performance and blade moments using the newly acquired test data and the comprehensive analysis CAMRAD II. Four low-speed conditions were studied, including hover (actually, low speed vertical climb), cruise (airplane mode), conversion, and helicopter mode. Mean and ½ peak-to-peak quantities (hpp) are correlated; time-history correlation for the helicopter condition is also included. The hover calculations proved useful in providing reality checks on the test hardware. The correlation is reasonable. The mean midspan flap banding moments are predicted very well. The trends (with C_T/σ) are largely captured, with some overprediction or underprediction (details in the paper). The time-history correlations (helicopter mode) show that, compared to the rolled-up wake (RW) model, the multiple-trailer wake model improves the correlation slightly; the collective is predicted well by the RW model, the lateral cyclic correlation is not good, and the longitudinal cyclic correlation is reasonable; the flap moment correlation is reasonable; the pitch link load and lag moment are underpredicted; and the torsion moment correlation is poor and needs further study.

NOTATION

40x80	40- by 80-Foot Wind Tunnel
A	rotor disk area, πR^2
C_T	rotor thrust coefficient, $T/\rho A V_t^2$
hpp	½ peak-to-peak
JVX	Joint Vertical Experimental proprotor
MTW	multiple-trailer wake
M_{tip}	tip Mach number
NFAC	National Full-Scale Aerodynamics Complex
R	rotor radius, ft
R*n*	wind tunnel test run number "*n*"
RW	rolled-up wake
T	rotor thrust, lb
TTR	Tiltrotor Test Rig
V	airspeed, knots
V_t	tip speed, ΩR
Yaw	TTR yaw angle; cruise is 0 deg and helicopter mode is 90 deg
μ	advance ratio, V/V_t
ρ	air density
σ	rotor solidity ratio
Ω	rotational speed

INTRODUCTION

A full-scale isolated proprotor test was recently conducted in the USAF National Full-Scale Aerodynamics Complex (NFAC) 40- by 80-Foot Wind Tunnel at NASA Ames Research Center. The test article was a 3-bladed research rotor, designated as the 699 rotor. The 699 is derived from the right-hand rotor of the AW609 and was manufactured by Bell Helicopter under contract to NASA. (The 699 was referred to as '609' in earlier publications, notably Ref. 1.) Figure 1 shows the TTR/699 installed in the NFAC 40- by 80-Foot Wind Tunnel test section. The TTR rotor axis is horizontal and the rig rotates in yaw on the wind tunnel turntable for conversion between airplane and helicopter mode testing. During wind tunnel checkout testing in August 2018, the TTR reached a maximum cruise (airplane mode, 0-deg yaw) airspeed of 273 knots. This is the highest airspeed ever achieved by a full-scale proprotor in any wind tunnel. This 699 proprotor performance and loads correlation study uses these newly acquired wind tunnel test data.

This paper represents the third analytical study for this test program, coming after pre-test predictions of 699 performance and loads (Ref. 1) and aeroelastic stability analyses of the TTR/699 installed in the 40- by 80-Foot Wind

Presented at the Vertical Flight Society's 75th Annual Forum & Technology Display, Philadelphia, PA, USA, May 13-16, 2019.

Tunnel (Ref. 2). Reference 3 presents an overview of the entire TTR/699 test program. Reference 4 addresses the acoustic testing of the TTR in the 40- by 80-Foot Wind Tunnel. For completeness it is noted that an earlier paper, Ref. 5, addressed the development and initial testing of the TTR.

Figure 1. TTR/699 installed in the USAF NFAC 40- by 80-Foot Wind Tunnel.

This paper presents an initial correlation of full-scale proprotor performance and loads. Four low-speed conditions are considered: hover (collective sweep and RPM sweep); low-speed cruise (91 knots); conversion (92 knots); and helicopter mode (70 knots). Details are given in the Results section.

As background, a limited amount of correlation data is available for full-scale proprotors. The 1971 report by Bell Helicopter (Ref. 6) contains XV-15 40x80 wind tunnel test data and theoretical predictions. A literature survey brought up several existing correlation studies, but these were either based on small-scale test data (for example, Refs. 7-8) or full-scale aircraft flight test data (for example, flight tests conducted by Bell Helicopter). Separately, the 2009 NASA study involving the JVX rotor is relevant (see Ref. 9). The JVX is similar to the 699 in size and aerodynamics, and is accordingly a good reference for performance calculations. In Ref. 1 (as mentioned above), pre-test reality checks of the current analytical model were made by comparing JVX and 699 predictions in hover and forward flight (airplane mode).

TTR Checkout Test

The checkout test was an integral part of the development of the TTR, whose purpose is to test advanced, full-scale proprotors in the NFAC (Refs. 3 and 5). The primary purpose of the just-completed checkout test was to demonstrate the operational capability of the TTR over a wide range of test conditions. A secondary goal was to safely collect as much research data as possible.

699 RESEARCH ROTOR

A brief description of the 699 research proprotor is provided here. The 3-bladed rotor has non-linear twist (47.5 deg) and square tips, the rotor diameter is 26 ft and the geometric solidity is 0.097. The rotor is stiff in-plane with a gimballed hub and yoke (flexbeam). The conversion and helicopter mode rpm is 569 (100%) and the airplane mode (cruise) rpm is 478 (84%). The highest 3P (3/rev) frequency is then 28.45 Hz.

The 699 rotor is based on the AW609 rotor, and was manufactured by Bell Helicopter under contract to NASA. The main differences between the research and flight rotors are listed below. The research rotor:

- Does not have deicing capability
- Has additional instrumentation
- Has a different pitch horn arrangement, specific to the TTR control system
- Does not have pendulum absorbers

See Ref. 3 for further details of the rotor and instrumentation.

ANALYTICAL MODEL

The rotorcraft comprehensive analysis CAMRAD II Release 4.9, Refs. 10-12, was used for the analytical predictions. Performance and loads calculations in Ref. 1 and in this study were performed for the 699 rotor with flexible blades and hub, including the gimbal, but with no fixed system flexibility.

The most recent CAMRAD II structural model for the 699 rotor is used in this study. Similar to the V-22 CAMRAD model (Ref. 13), a dual load-path model is used for the 699 rotor. The yoke (flexbeam) and the blade form the two load paths. The CAMRAD II aerodynamic model requires airfoil tables, which were provided by Bell Helicopter as C81 tables. The rotor model includes the gimbal and swashplate degrees of freedom. The blade is modeled as an elastic beam with elastic beam elements, with two degrees of freedom each for torsion, flap and lag bending. In the trim calculations, 12 elastic blade modes are used (torsion, flap and lag).

For the performance and loads predictions (here and in Ref. 1), the CAMRAD II rolled-up wake (RW) model is used. For time-history predictions which require more detailed wake modeling, the current study also uses the CAMRAD II multiple trailer wake (MTW) model (Ref. 14).

The analytical model used here is identical to that of Ref. 1 (and Ref. 2, the aeroelastic stability study). The difference between Ref. 1 and this paper is that the analytical operating conditions presented here are matched to the test conditions actually achieved; this paper additionally contains time-history correlations using the RW and MTW wake models.

The analysis trim procedures are now described. For hover, either the rpm is varied with fixed collective or the collective is varied with fixed rpm. For cruise, the collective is varied (thrust sweep) with fixed rpm. For the helicopter and conversion conditions, the current trim procedure differs from that of Ref. 1; the present study uses the Ref. 2 trim procedure — for a given airspeed, the rotor is trimmed to zero 1P flapping, while increasing the collective (no thrust trim). This

simulates the procedure followed during a typical wind tunnel test run.

For the hover calculations presented in this paper, the following caveat from Ref. 5 (and Ref. 3) is relevant: "In the NFAC, true hover is challenging at full scale. The effects of tunnel walls cannot be completely avoided in the 40x80 test section. Furthermore, the rotor's induced velocity continues around the tunnel circuit without completely dissipating, so the test conditions are actually low-speed vertical climb."

Finally, the current predictions use a comprehensive analysis with lifting line theory, with no wind tunnel wall effects (a completely isolated proprotor is considered). Inclusion of wall effects and the use of higher order airloads from a CFD analysis may improve the current correlations.

RESULTS

Initial correlations of full-scale proprotor performance and loads are presented in this paper. The following four types of low-speed correlations are covered:

- Pre "wind on" hover reality checks (wind tunnel fans not operating)
    - Varying rpm hover predictions were used to check the blade moment strain gages, especially, the inboard safety of flight gages.
    - Hover predictions were used to verify that the analytical and test collective pitch values were reasonably close to each other.
- Cruise (0-deg yaw, V=91 knots)
- Conversion (45-deg yaw, V=92 knots)
- Helicopter mode time-history predictions (75-deg yaw, V=70 knots)

Only mean quantities are correlated for the hover and cruise conditions since the loads are predominantly steady. The ½ peak-to-peak (hpp) quantities are added for the conversion and helicopter modes, and time-histories are also looked at for the helicopter mode.

To achieve a specified test operational condition, the experimental procedure followed during a test run was to set the tip Mach number M_{tip} and advance ratio μ. For CAMRAD II calculations involving collective (thrust) sweeps, the analytical procedure followed was to input an average rpm (Ω) and V based on their respective test values; this was done for the hover, cruise, and conversion modes that involved parametric sweeps. For the single condition helicopter mode, the analysis matched the following test quantities: density, temperature, Ω, TTR yaw, airspeed, and C_T/σ.

Results are shown for the thrust, torque, blade and flexbeam (yoke) bending moments, blade torsion moments, and pitch link loads. (For cruise, results for only the mean thrust, torque, pitch link load, and midspan bending moments are shown.) For conversion and helicopter mode, the results also include cyclic trim angles. The conversion mode results include mean and ½ peak-to-peak (hpp) quantities; the helicopter mode results additionally include load time histories. Finally, for cases which involve hpp correlation, the figures have "hpp" in their legends; if the figure legend does not contain "hpp" then this implies a mean quantity is being correlated.

The blade stations used for correlation and their corresponding radial locations are listed below:

inboard:	0.20R
midspan:	0.45R
outboard:	0.75R
yoke inboard:	0.08R
yoke outboard:	0.11R

The flap and lag moments refer to the bending moments about the local section normal and chord axes, respectively. The 699 rotor hub has pitch bearings; the pitch bearings and the gimbal isolate the yoke from torsion loads. In this paper, only yoke bending moment correlations are shown.

The sign convention is as follows:

pitch link load:	+ tension
flap bending moment:	+ tip bent up
lag bending moment:	+ tip bent toward trailing edge
torsion moment:	+ blade twisted leading edge up

In the figures, except for the thrust which is plotted vs. collective, all other quantities are plotted vs. C_T/σ to eliminate any dependency on exact collective trim.

Hover (Vertical Climb)

As noted earlier, a true hover test condition is not possible in the NFAC 40x80 test section due to wall effects and tunnel circuit recirculating flow, and the current results must be viewed in this light. Two sets of hover results are shown in this paper: a) varying rpm, nominal pitch and b) constant rpm, varying collective pitch.

Varying rpm, nominal collective. For the varying rpm results, the test rpm range was 82 to 569 (100%, the hover rpm) at collective=5 deg. The analytical procedure was as follows: for a given rpm, vary the collective in order to match the measured thrust. Also, mean values of the measured test section airspeed (VKTS) were used as inputs in the CAMRAD II predictions. Two sets of analytical results are thus shown: one with zero airspeed ("predicted, zero VKTS") and the second with the average measured airspeed ("predicted, test VKTS"). Figures 2-9 show the results, all vs. rpm. Figure 2 shows the measured VKTS and the corresponding averaged airspeed variation used as input in CAMRAD II. Note that the test data in Figure 2 is from a single run very early in the TTR test program (Run 59) and the large scatter indicates a worst case run; subsequent runs show less scatter. In Run 59, the rpm was first increased and then decreased (there is hysteresis in the data).

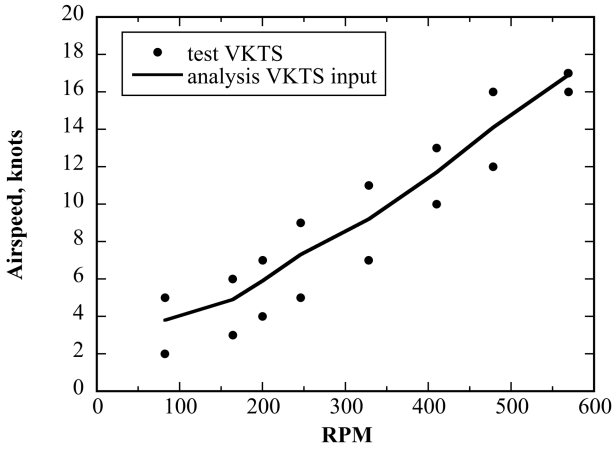

Figure 2. Measured test section airspeed VKTS and analysis input, vertical climb, collective=5 deg.

Figure 3 shows the measured and analytically matched thrust variations. The rest of the correlation results for this varying rpm case are as follows:

Figure 4: torque
Figure 5: pitch link load
Figure 6: flap moment (inboard, midspan, outboard)
Figure 7 yoke flap moment (inboard, outboard)
Figure 8: lag moment (inboard, midspan, outboard)
Figure 9: yoke lag moment (inboard, outboard).

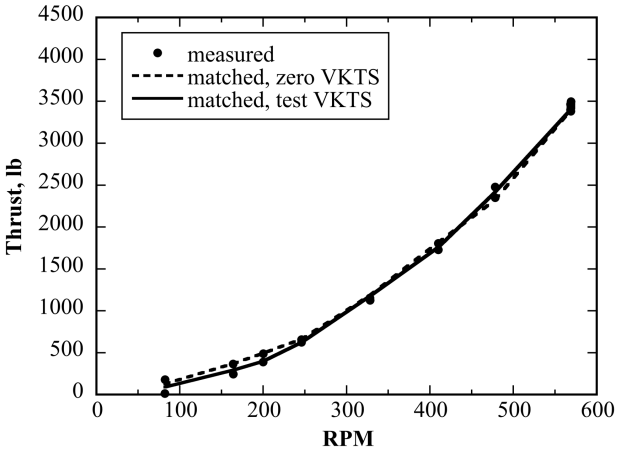

Figure 3. Measured thrust and matched analytical thrust.

Figures 4-9 show that the current predictions capture the trends with rpm. The correlation for the important safety of flight gages (inboard flap and lag gages, Figures 6a and 8a) is considered good, and also sufficient to verify that the installed blade strain gages are functioning as desired. The overall level of correlation is satisfactory for this varying rpm scenario and is considered to have served its purpose of helping in checking out the strain gages.

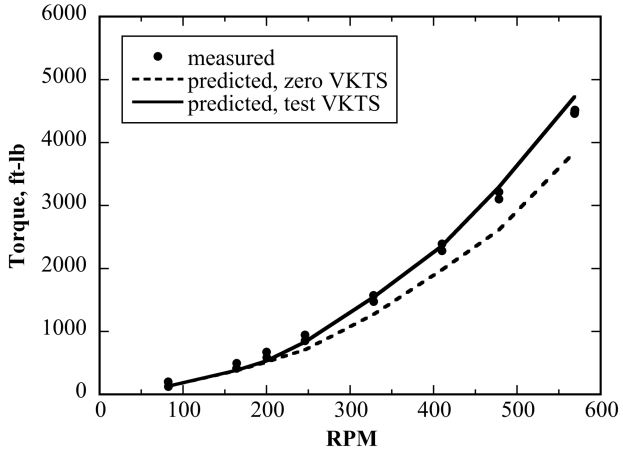

Figure 4. Measured and predicted torque.

Specific observations on the correlation are as follows. The introduction of the measured airspeed improves all correlation except the inboard lag moments, which shows that CAMRAD II accurately captures this effect (Figures 4-9). The torque and pitch link load correlations are good (Figures 4-5). The safety of flight flap correlation is good (within the inboard data scatter, Figure 6a). The yoke flap moment correlation is reasonable (Figure 7). The predicted lag moments capture the trends but not the magnitudes (Figures 8-9). The large twist of the 699 changes the orientation of the lag gages relative to the tip path plane, hence the inboard and outboard moments do not have the same trend (the inboard moment increases with rpm and the outboard moment decreases with rpm, Figure 8).

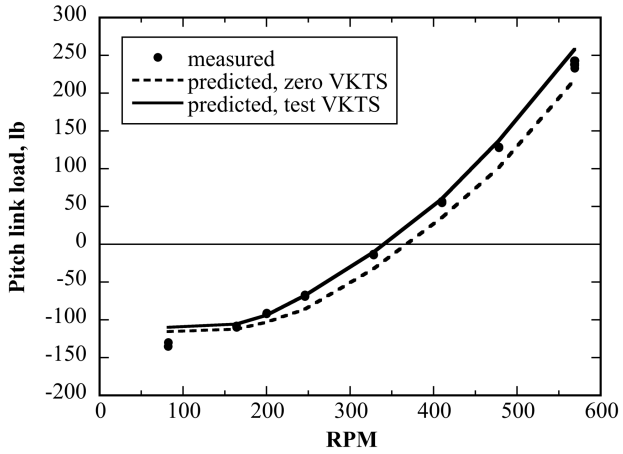

Figure 5. Measured and predicted pitch link load.

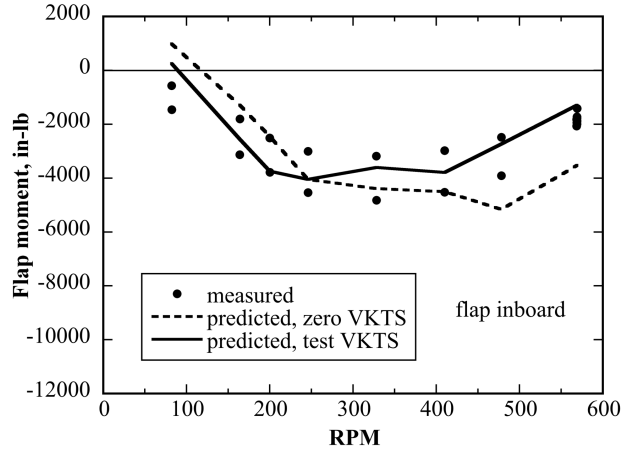

(a) Inboard

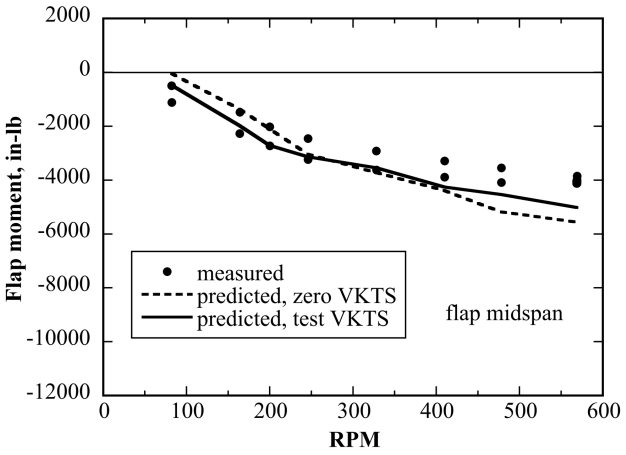

(b) Midspan

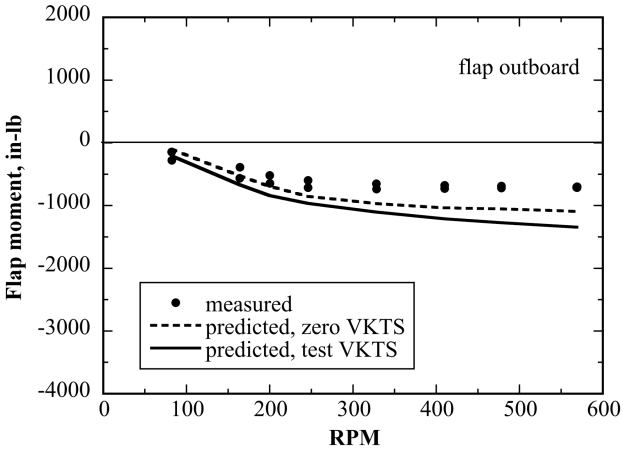

(c) Outboard

Figure 6. Measured and predicted blade flap moments (inboard, midspan, outboard).

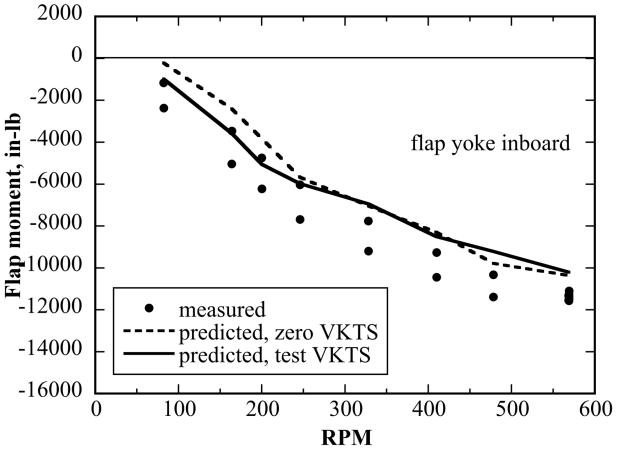

(a) Yoke inboard

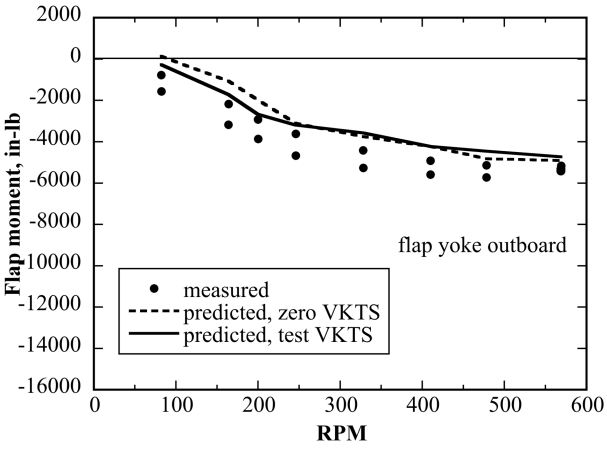

(b) Yoke outboard

Figure 7. Measured and predicted yoke flap moments (inboard, outboard).

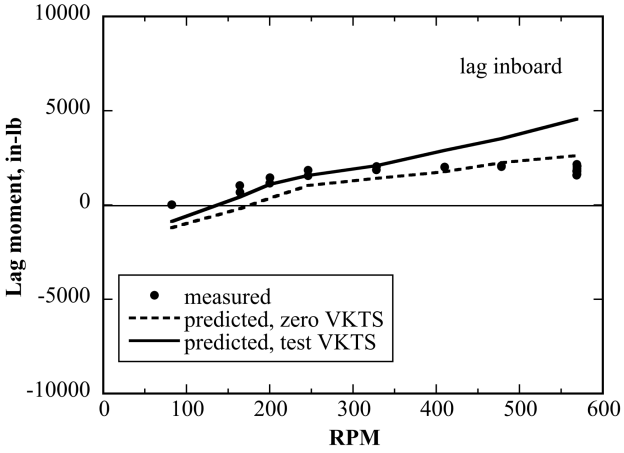

(a) Inboard

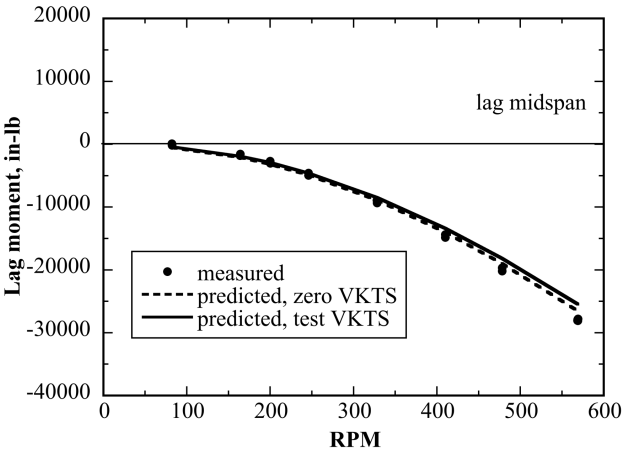

(b) Midspan

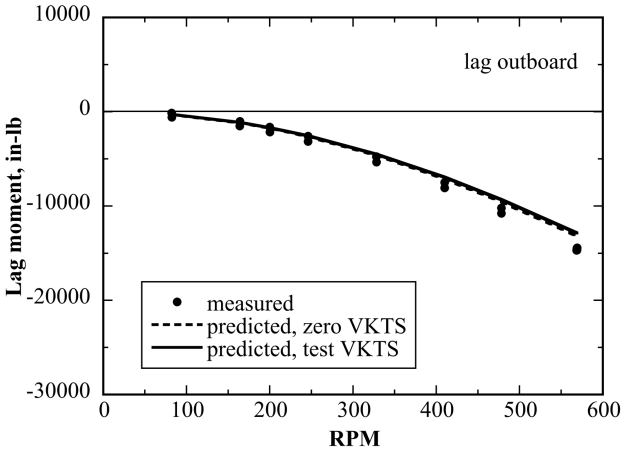

(c) Outboard

Figure 8. Measured and predicted blade lag moments (inboard, midspan, outboard).

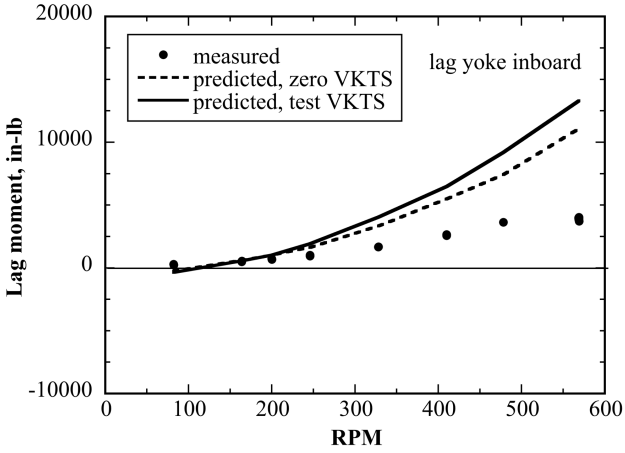

(a) Yoke inboard

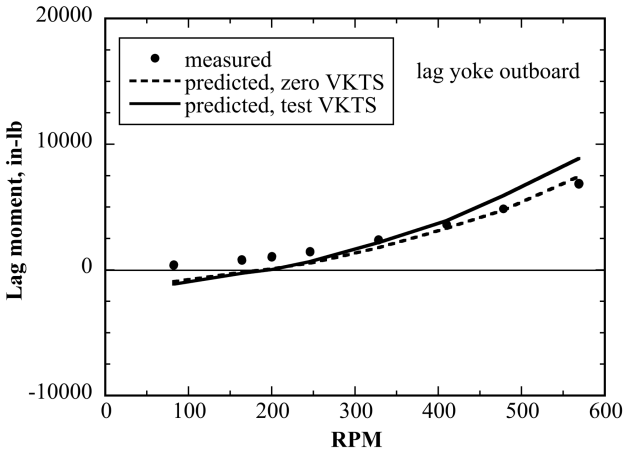

(b) Yoke outboard

Figure 9. Measured and predicted yoke lag moments (inboard, outboard).

Constant rpm, varying collective. The second set of hover predictions involved a constant shaft speed Ω=569 with varying collective. Here, two groups of wind tunnel hover test runs are involved: Runs 59-61 and Runs 62-63. The difference between the two run groups is that the first used the standard NFAC 40x80 closed circuit configuration and the second had the TTR oriented 180 deg with respect to the first configuration. Both groups entailed non-zero airspeeds in the test section, but, compared to the first group, the second group had *lower* test section airspeeds (VKTS); this can be seen in Figure 10 which shows measured airspeed vs. collective for runs R59-R61 and R62-R63.

Analytically, three sets of predictions were obtained: hover (zero VKTS) and vertical climb with averaged VKTS from R61 and separately from R63. Figures 11 and 12 show the resulting thrust and torque correlations with the three analytical variations ("predicted, hover", "predicted, R61 airspeed", and "predicted R63 airspeed"). Figure 11 clearly shows that introducing a non-zero airspeed improves the

thrust correlation. For the torque (Figure 12), the current results show no important discernible difference at this scale. In any case, the purpose of this exercise was to make a reality check on the test and analytical collective pitch values. Figure 11 (thrust correlation) demonstrates that the test and analytical collectives were within roughly ± 1 deg of each other. Recall that this set of calculations was performed just prior to "wind on" (forward flight) testing and turned out to be useful for verifying the calibration of the pitch measurement hardware.

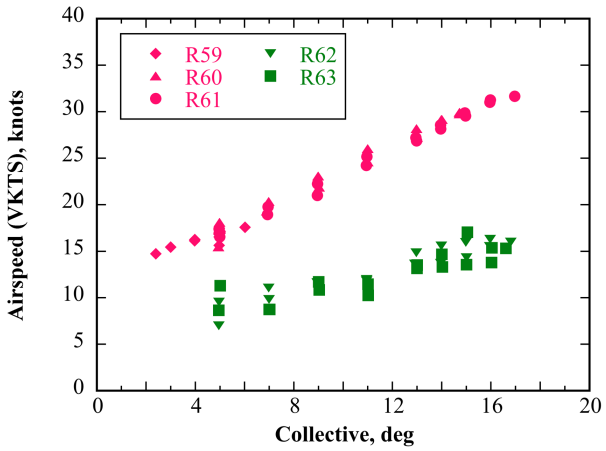

Figure 10. Measured test section airspeed VKTS for two run groups.

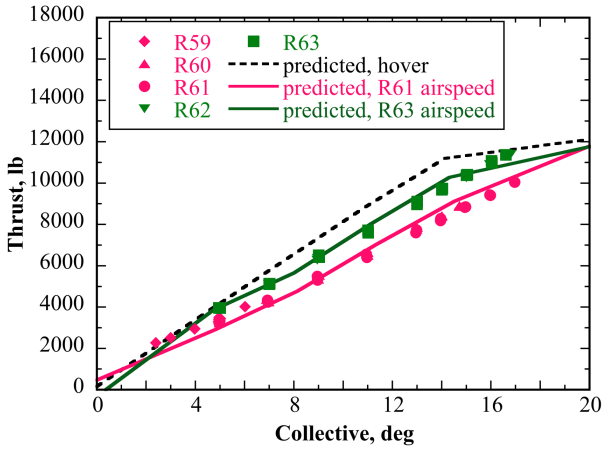

Figure 11. Measured and predicted thrust.

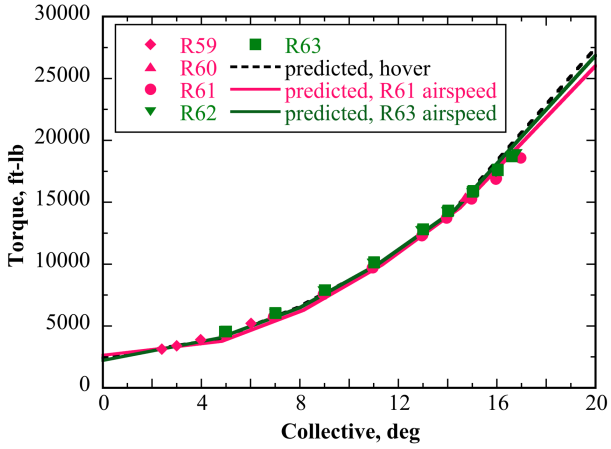

Figure 12. Measured and predicted torque.

Cruise (airplane mode)

Figure 13 shows the thrust correlation vs. collective for this axial flow condition. Figures 14-16 show the torque, pitch link load, and midspan blade flap and lag bending moments, all vs. the thrust coefficient C_T/σ. The operational parameters are: Ω=485, V=91 knots, μ=0.233. The correlation at this low cruise speed is reasonable.

Specifically, the thrust correlation (Figure 13) shows underprediction at low collective; the torque is slightly underpredicted at higher C_T/σ (Figure 14). Both types of discrepancies need further study (as noted earlier, this could include inclusion of wind tunnel wall effects). The pitch link load is underpredicted (Figure 15), the midspan flap bending moment correlation is good (Figure 16a), and the lag moment is overpredicted (Figure 16b).

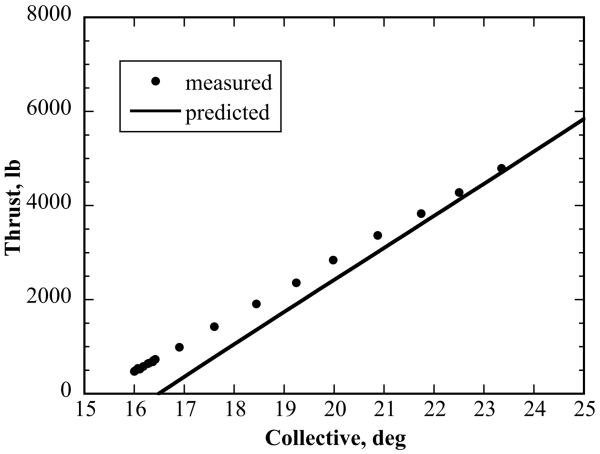

Figure 13. Measured and predicted thrust vs. collective, cruise, 0-deg yaw, Ω=485, V=91 knots, μ=0.233.

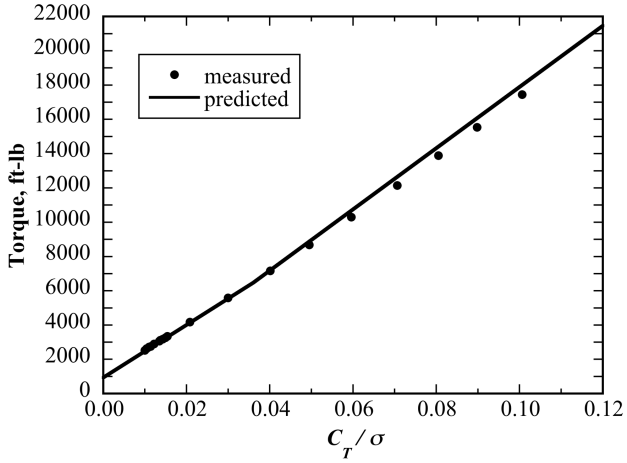

Figure 14. Measured and predicted torque, cruise, 0-deg yaw, Ω=485, V=91 knots, μ=0.233.

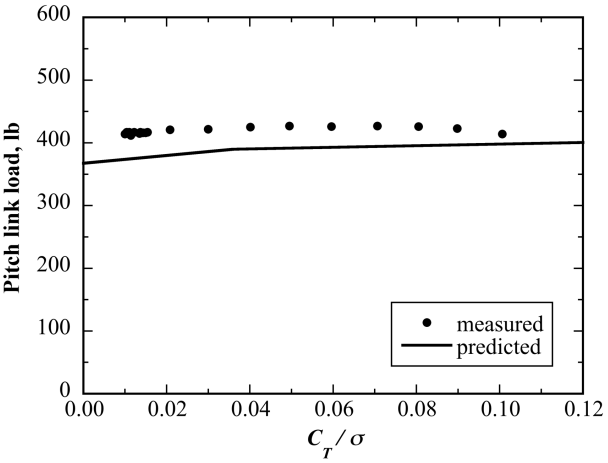

Figure 15. Measured and predicted pitch link load, cruise, 0-deg yaw, Ω=485, V=91 knots, μ=0.233.

Conversion

For conversion, results for all blade stations are shown. Mean and ½ peak-to-peak (hpp) quantities are correlated. The TTR was oriented at 45-deg yaw and Ω=569, V=92 knots, μ=0.200.

Figure 17 shows the conversion thrust vs. collective. Figures 18-28 show the rest of the conversion results, all vs. C_T/σ. Figures 18-19 show the rotor performance parameters: trim cyclics and torque. Figure 18 shows the correlation for the cyclics required to trim to zero 1P flapping, where Lat=lateral cyclic trim and Long=longitudinal cyclic trim. Figure 19 shows the torque correlation. Figure 20 shows the pitch link load correlation. Figures 21-28 show the blade and yoke moment correlations (flap: mean, hpp, Figures 21-24, and lag: mean, hpp, Figures 25-28).

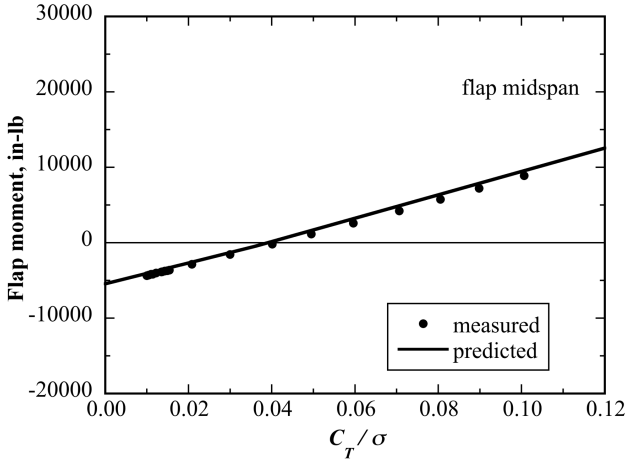

(a) Flap

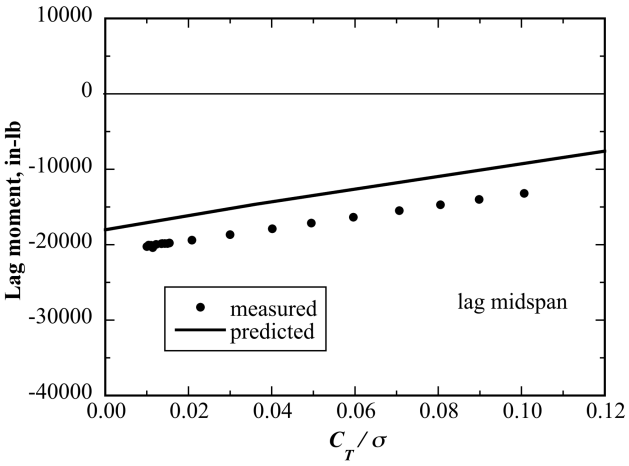

(b) Lag

Figure 16. Measured and predicted lag bending moment, cruise, 0-deg yaw, Ω=485, V=91 knots, μ=0.233.

Specific observations on the conversion correlation are as follows. The thrust correlation is reasonable, with underprediction at lower collective (Figure 17) and this needs further study. The trim cyclics correlation is good (Figure 18). The torque correlation is excellent (Figure 19). The pitch link load correlation is reasonable (the trends are largely captured), the mean load is predicted well but the hpp load is underpredicted (Figure 20). For the flap moment, the trends are captured (except for the yoke moments), there is overprediction or underprediction, and the mean midspan moment correlation is excellent (Figures 21-24). For the lag moment, the trends are captured, the mean loads are soverpredicted, and the hpp correlation is reasonable (Figures 25-28). The current 45-deg yaw conversion correlation is reasonable, with the analysis capturing most of the trends.

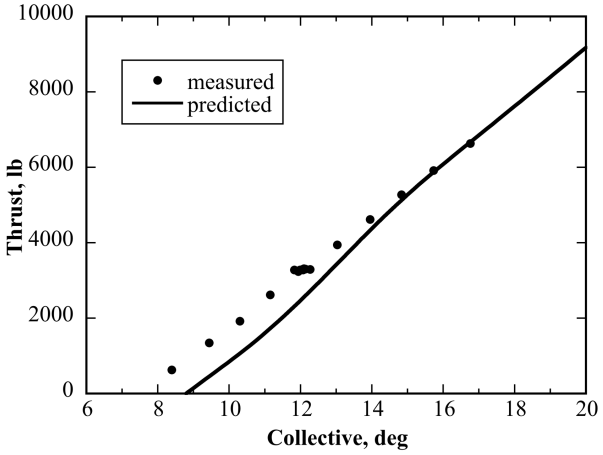

Figure 17. Measured and predicted thrust vs. collective, conversion, 45-deg yaw, Ω=569, V=92 knots, μ=0.200.

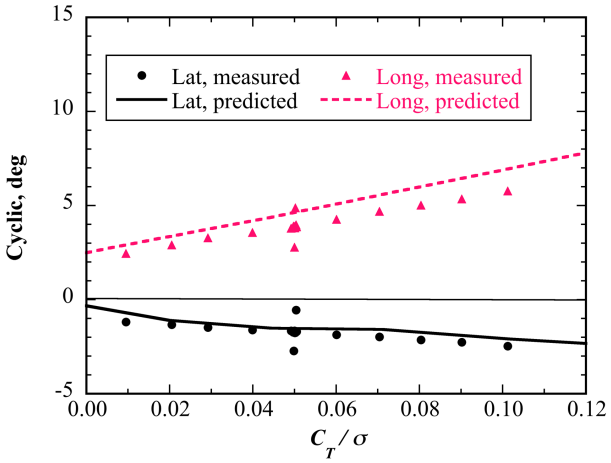

Figure 18. Measured and predicted cyclics, conversion, 45-deg yaw, Ω=569, V=92 knots, μ=0.200.

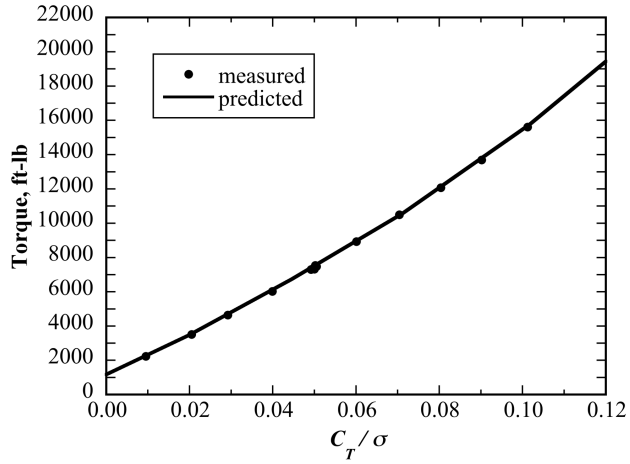

Figure 19. Measured and predicted torque, conversion, 45-deg yaw, Ω=569, V=92 knots, μ=0.200.

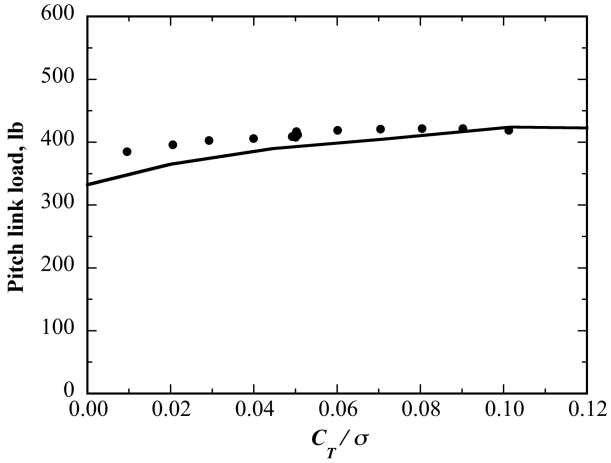

(a) Mean

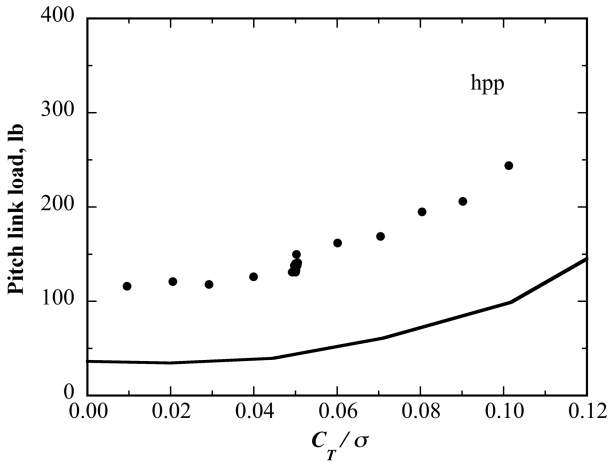

(b) ½ peak-to-peak (hpp)

Figure 20. Measured and predicted mean and hpp pitch link load, conversion, 45-deg yaw, Ω=569, V=92 knots, μ=0.200.

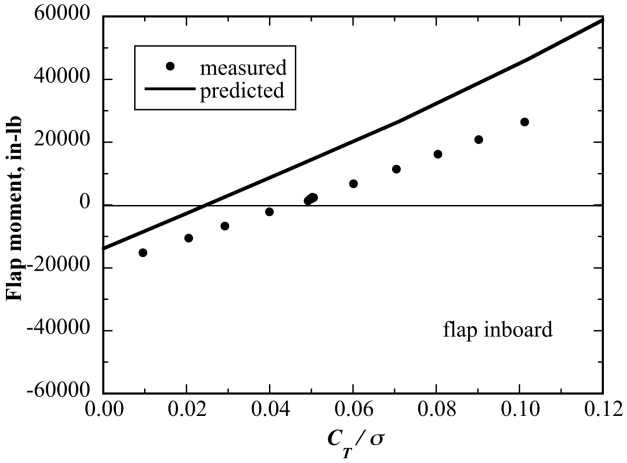

(a) Inboard (mean)

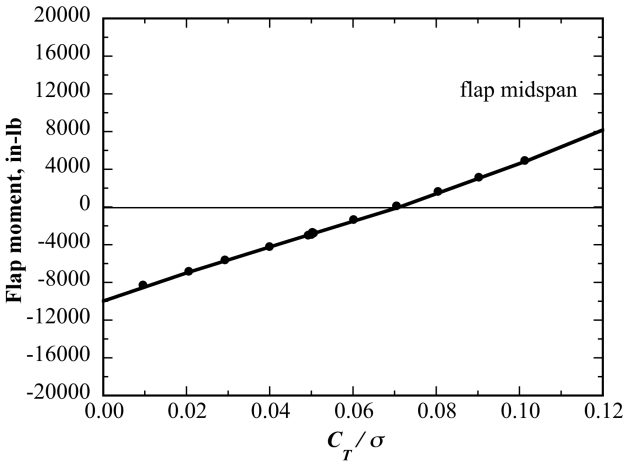

(b) Midspan (mean)

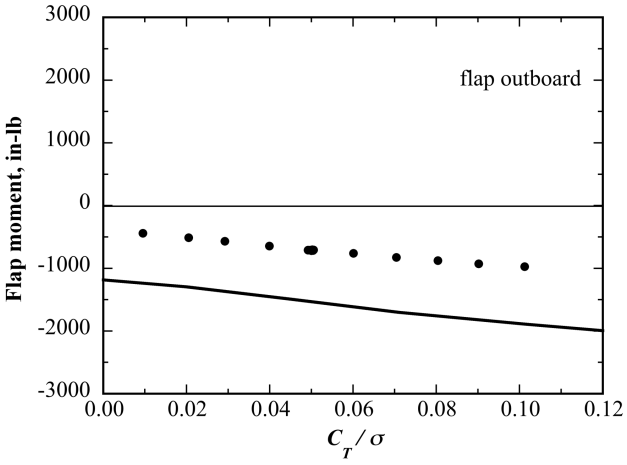

(c) Outboard (mean)

Figure 21. Measured and predicted mean flap bending moments, conversion, 45-deg yaw, Ω=569, V=92 knots, μ=0.200.

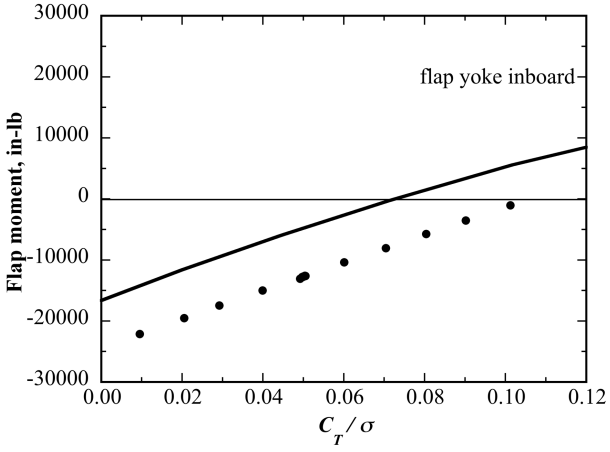

(a) Yoke inboard (mean)

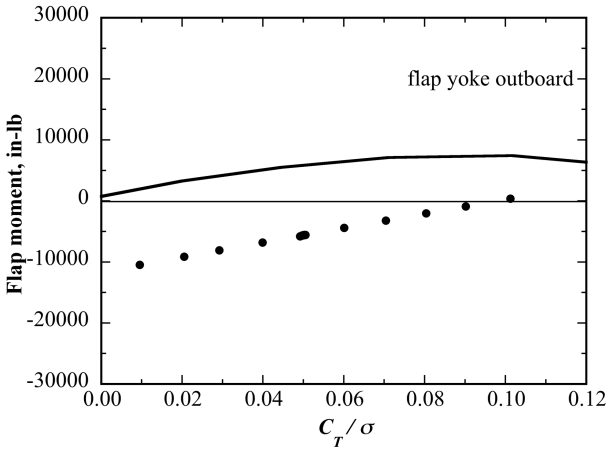

(b) Yoke outboard (mean)

Figure 22. Measured and predicted mean yoke flap bending moments, conversion, 45-deg yaw, Ω=569, V=92 knots, μ=0.200.

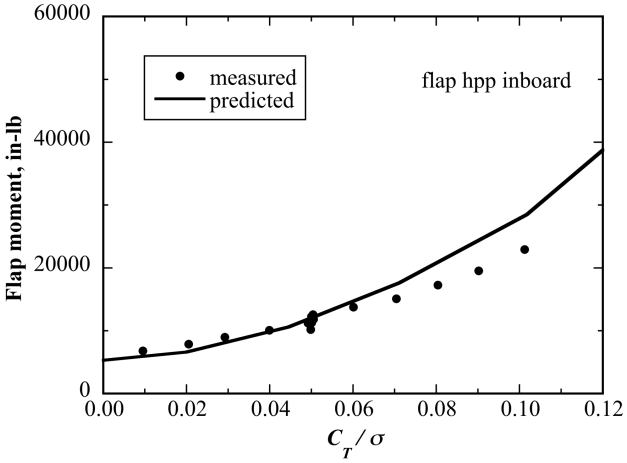

(a) Inboard (hpp)

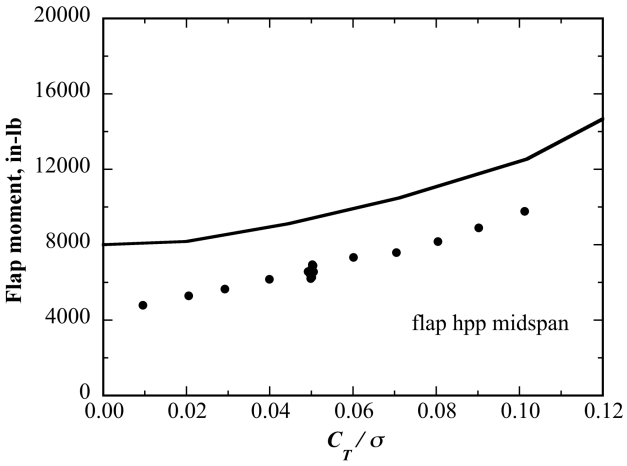

(b) Midspan (hpp)

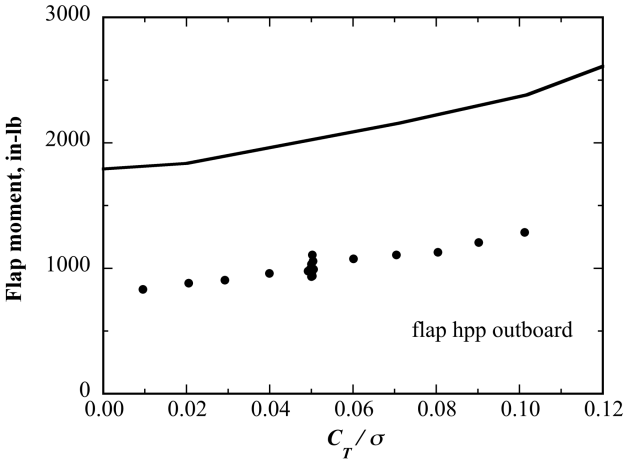

(c) Outboard (hpp)

Figure 23. Measured and predicted hpp flap bending moments, conversion, 45-deg yaw, Ω=569, V=92 knots, μ=0.200.

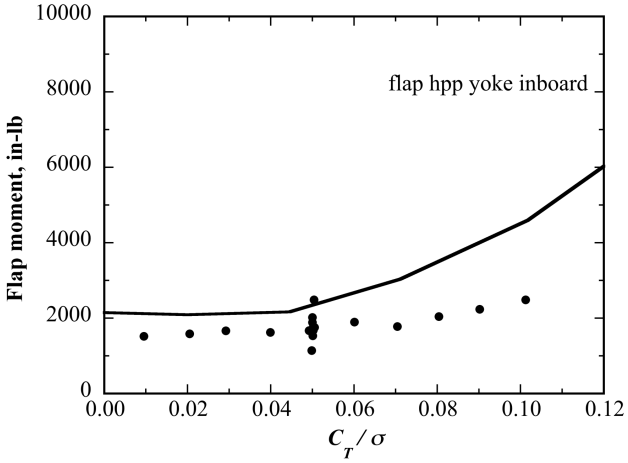

(a) Yoke inboard (hpp)

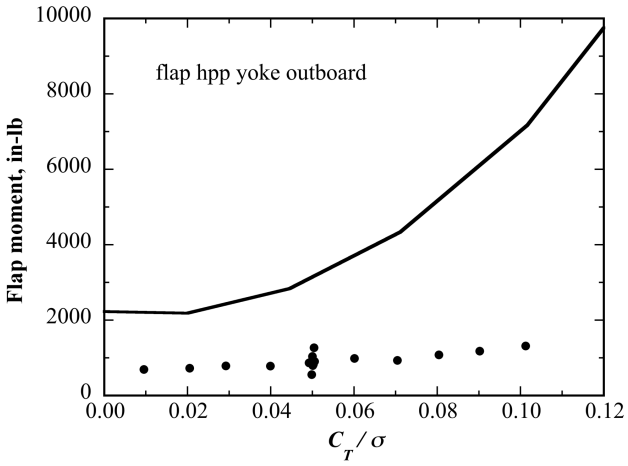

(b) Yoke outboard (hpp)

Figure 24. Measured and predicted hpp yoke flap bending moments, conversion, 45-deg yaw, Ω=569, V=92 knots, μ=0.200.

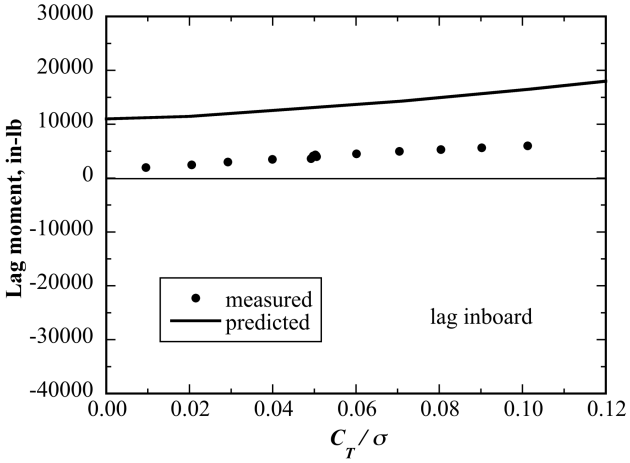

(a) Inboard (mean)

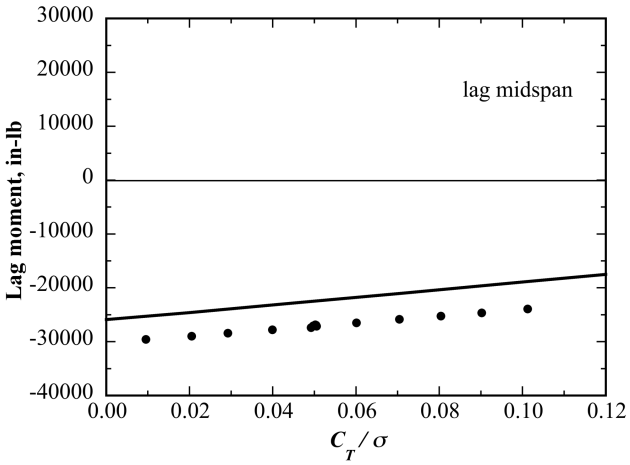

(b) Midspan (mean)

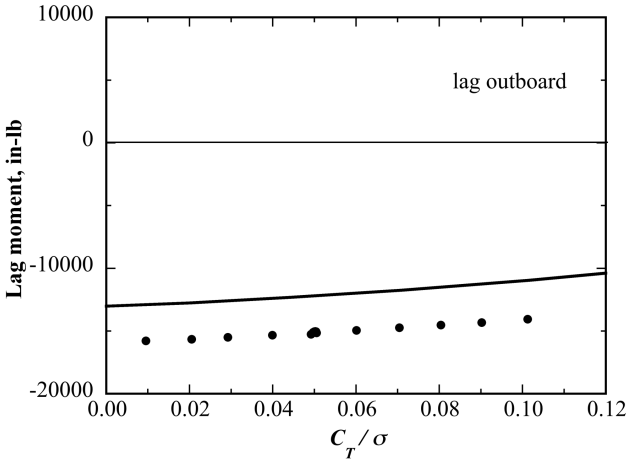

(c) Outboard (mean)

Figure 25. Measured and predicted mean lag bending moments, conversion, 45-deg yaw, Ω=569, V=92 knots, μ=0.200.

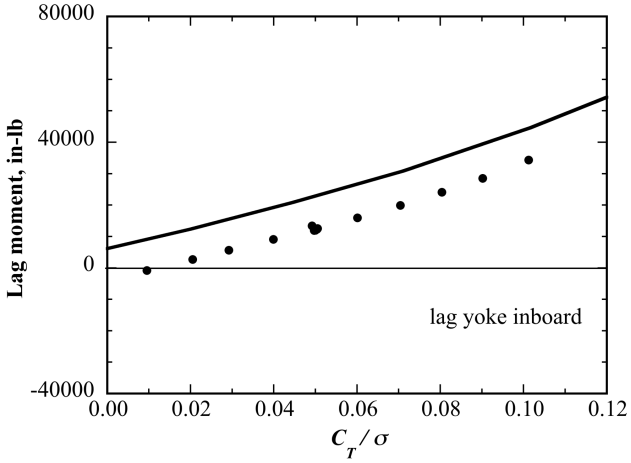

(a) Yoke inboard (mean)

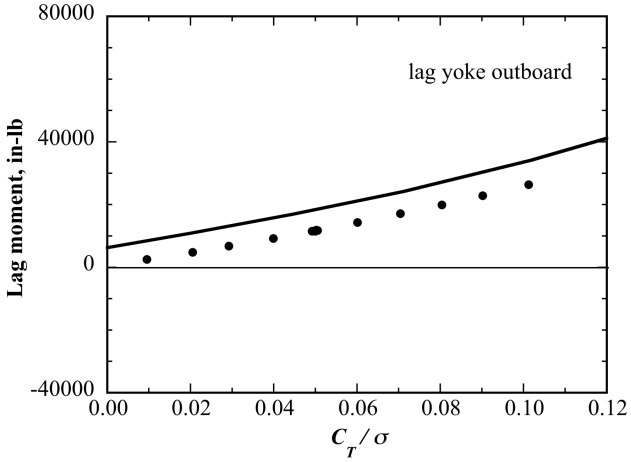

(b) Yoke outboard (mean)

Figure 26. Measured and predicted mean lag yoke bending moments, conversion, 45-deg yaw, Ω=569, V=92 knots, μ=0.200.

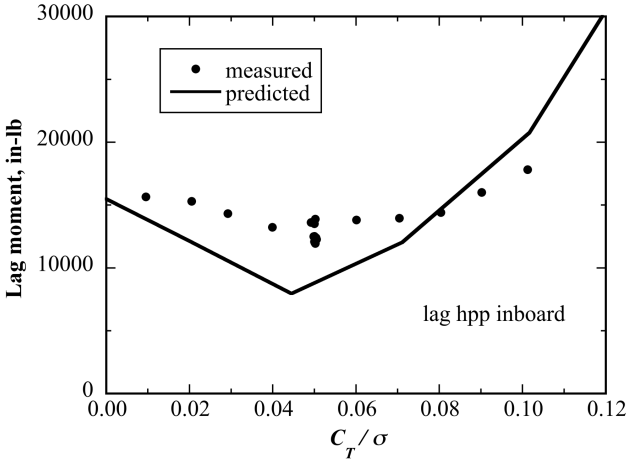

(a) Inboard (hpp)

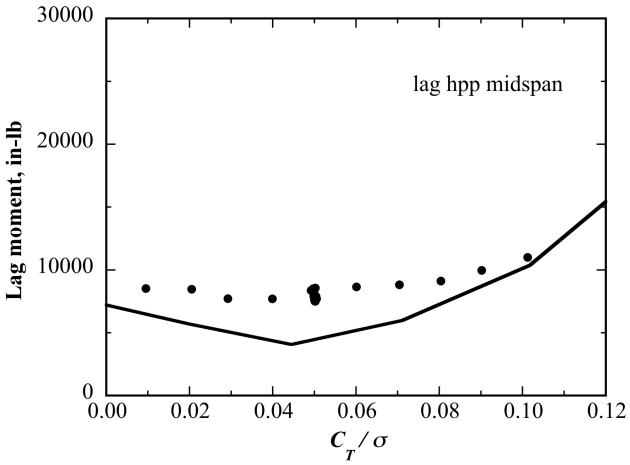

(b) Midspan (hpp)

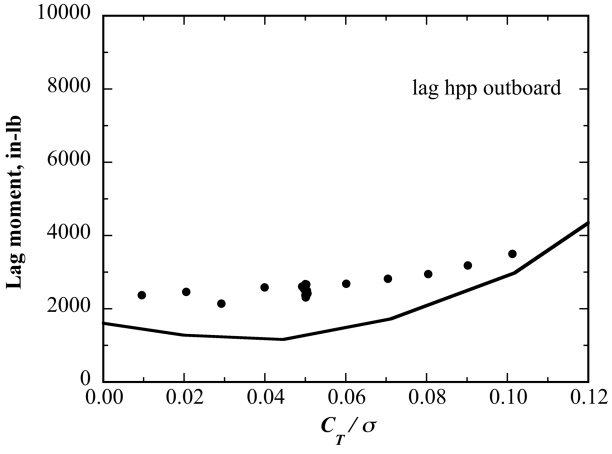

(c) Outboard (hpp)

Figure 27. Measured and predicted hpp lag bending moments, conversion, 45-deg yaw, Ω=569, V=92 knots, μ=0.200.

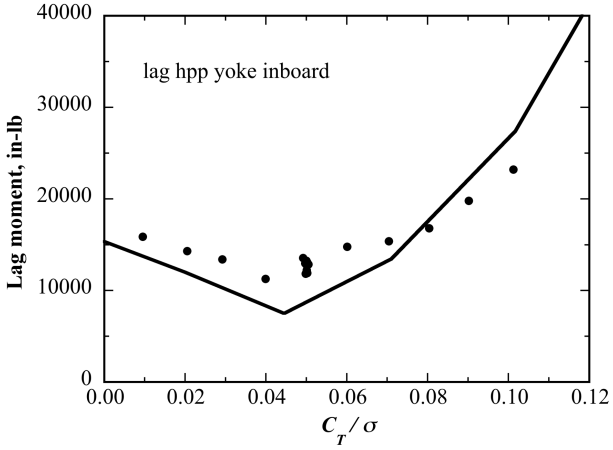

(a) Yoke inboard (hpp)

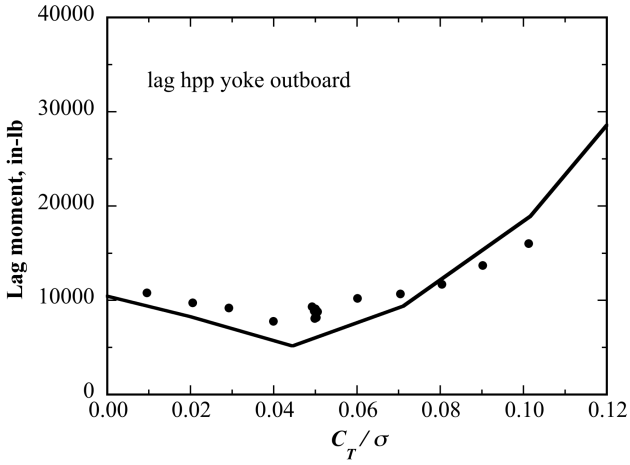

(b) Yoke outboard (hpp)

Figure 28. Measured and predicted hpp yoke lag bending moments, conversion, 45-deg yaw, Ω=569, V=92 knots, μ=0.200.

Helicopter Mode

Correlations of the mean and hpp quantities are shown in this section. The time histories of the 699 rotor loads are also looked at in this section. The time histories were obtained as a reality check to ascertain whether reasonable correlation could be obtained under the current analytical assumptions.

A low-speed helicopter mode condition with the rotor oriented 15 deg into the wind was selected. This condition is consistent with the small-scale results reported in Refs. 7-8. The present full-scale operating condition is: 75-deg yaw, Ω=573, V=70 knots, μ=0.151, and C_T/σ =0.081. The rotor was trimmed to C_T/σ and zero 1P flapping. Correlations with the rolled-up wake (RW) model (single tip vortex) and the multiple-trailer wake (MTW) model (multiple far wake trailers) are shown.

Mean and ½ peak-to-peak (hpp) correlation. The correlation for the mean quantities is shown in Figures 29-31 and the hpp correlation is shown in Figures 32-35, all as column charts. Figure 29 shows the measured and the corresponding analytically trimmed C_T/σ (and the resulting thrust). The torque is shown in Figure 30 and the trim controls are shown in Figure 31. The hpp blade (and yoke) flap and lag moment correlations are shown in Figures 32-33, respectively. The hpp pitch link load correlation is shown in Figure 34 and the hpp blade torsion moment correlation is shown in Figure 35.

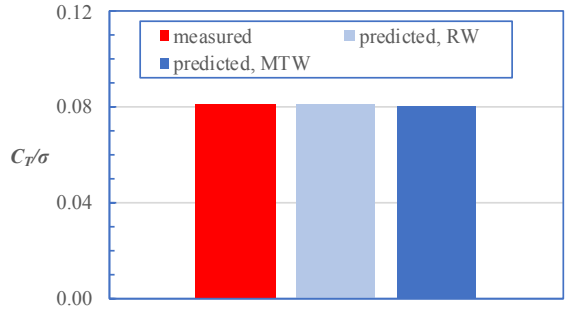

(a) C_T/σ

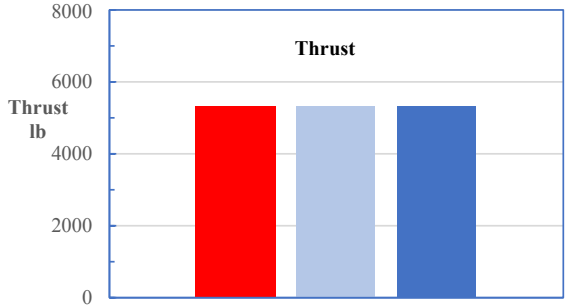

(b) Thrust

Figure 29. Measured and analytically trimmed C_T/σ and thrust, 75-deg yaw, Ω=573, V=70 knots, μ=0.151, C_T/σ =0.081.

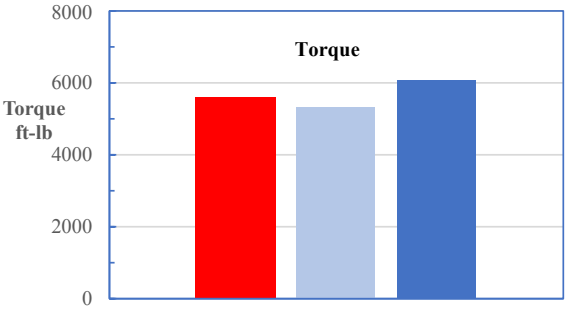

Figure 30. Measured and predicted torque, 75-deg yaw, Ω=573, V=70 knots, μ=0.151, C_T/σ =0.081.

Specific observations are as follows. The torque is slightly underpredicted by the RW model but overpredicted by the MTW model (Figure 30). The collective is predicted well by the RW model, the lateral cyclic correlation is not good, and the longitudinal cyclic correlation is reasonable (Figure 31). The midspan and outboard blade flap moment correlations are reasonable, and the inboard yoke flap moment is predicted well (Figure 32). The lag moment is underpredicted, with MTW improving the yoke correlation slightly (Figure 33). The pitch link load is underpredicted, with MTW improving the correlation slightly (Figure 34). The torsion moment correlation is poor and needs further study (Figure 35).

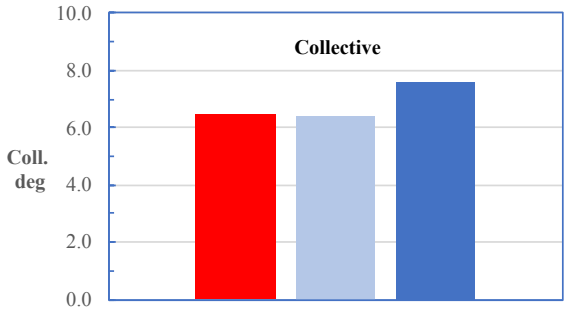

(a) **Collective**

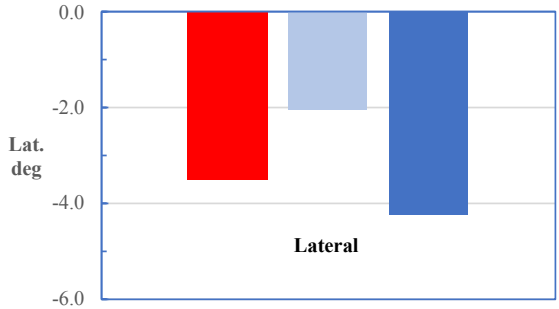

(b) Lateral cyclic

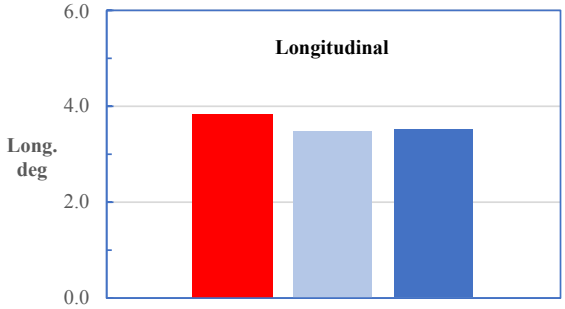

(b) Longitudinal cyclic

Figure 31. Measured and predicted control angles, 75-deg yaw, Ω=573, V=70 knots, μ=0.151, C_T/σ =0.081.

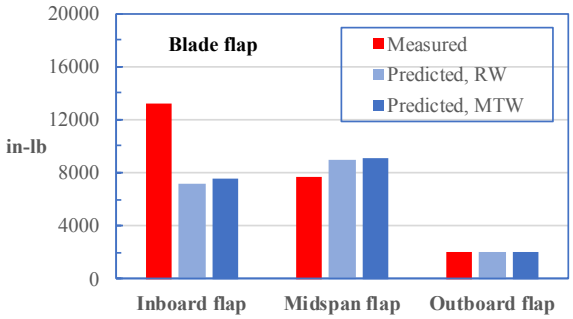

(a) Blade moments

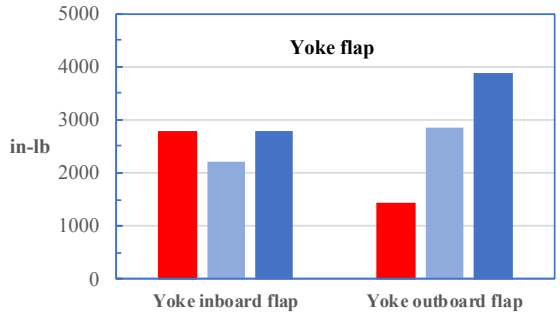

(b) Yoke moments

Figure 32. Measured and predicted blade and yoke hpp flap moments, 75-deg yaw, Ω=573, V=70 knots, μ=0.151, C_T/σ =0.081.

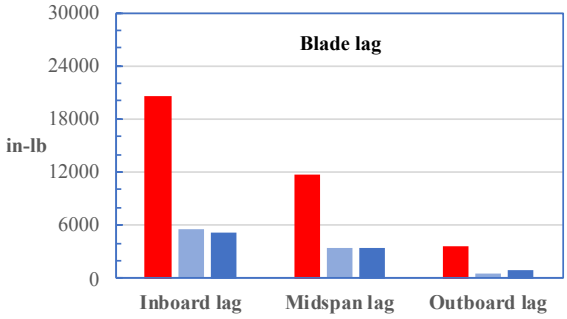

(a) Blade moments

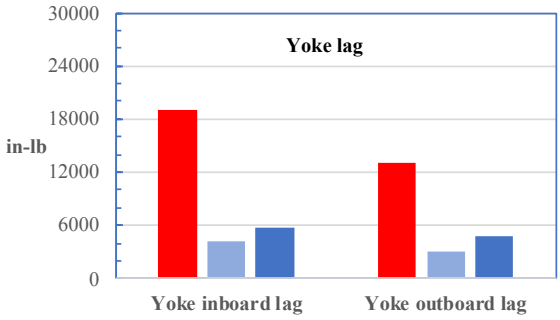

(b) Yoke moments

Figure 33. Measured and predicted blade and yoke hpp lag moments, 75-deg yaw, Ω=573, V=70 knots, μ=0.151, C_T/σ =0.081.

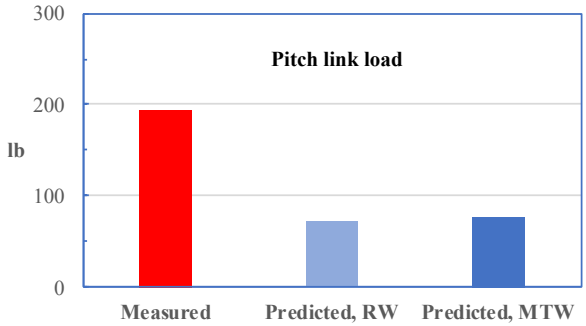

Figure 34. Measured and predicted hpp pitch link load, 75-deg yaw, Ω=573, V=70 knots, μ=0.151, C_T/σ =0.081.

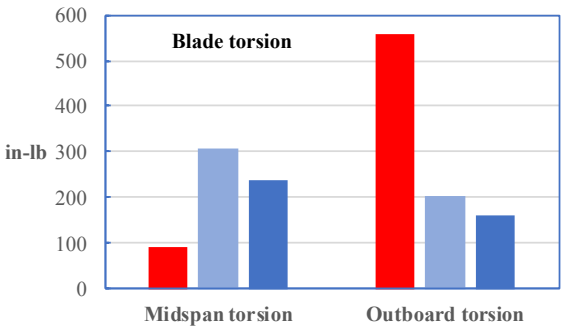

Figure 35. Measured and predicted hpp torsion moments, 75-deg yaw, Ω=573, V=70 knots, μ=0.151, C_T/σ =0.081.

Time-history correlation. Figures 36-39 show the time-history correlations for the blade and yoke bending moments, Figure 40 shows the pitch link load correlation, and Figure 41 shows the blade torsion moments for this helicopter mode.

Specific observations on the current isolated rotor time-history correlation are as follows (here, the performance of the RW and MTW models is being compared). Broadly, the blade flap moment correlation is good, with the phase and magnitude being captured better by the MTW model (Figures 36 and 38). The lag moment magnitude is underpredicted with the MTW model improving the phase correlation, but the 2/rev component in the yoke moments is not captured (Figures 37 and 39). The analysis picks up some of the higher frequency content in the pitch link load time-history, with magnitude underpredicted, and MTW improves the phase correlation slightly (Figure 40. The torsion moment correlation needs further study (Figure 41).

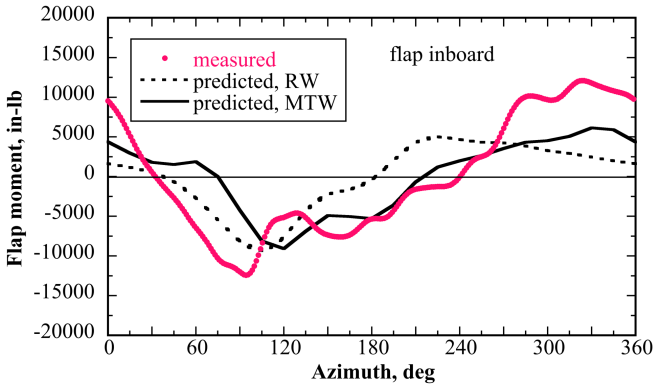

(a) Inboard

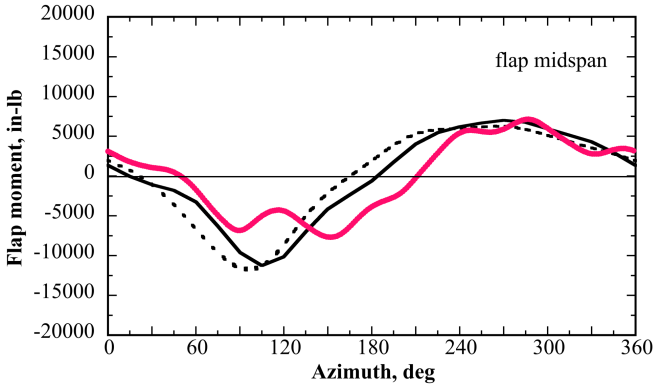

(b) Midspan

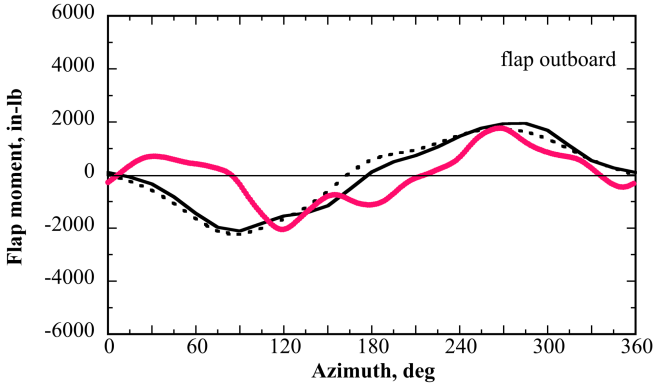

(c) Outboard, scale change

Figure 36. Flap moment time histories, helicopter mode, 75-deg yaw, Ω=573, V=70 knots, μ=0.151, C_T/σ =0.081

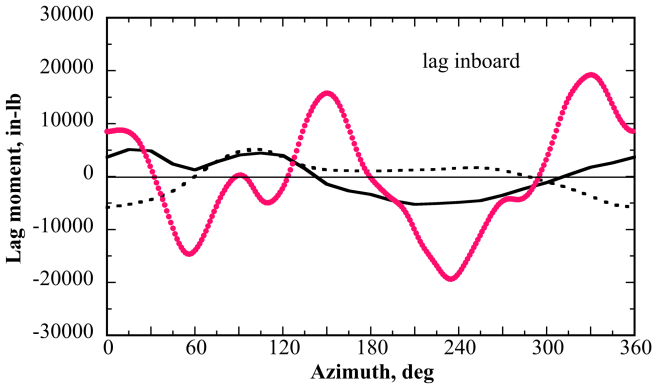

(a) Inboard

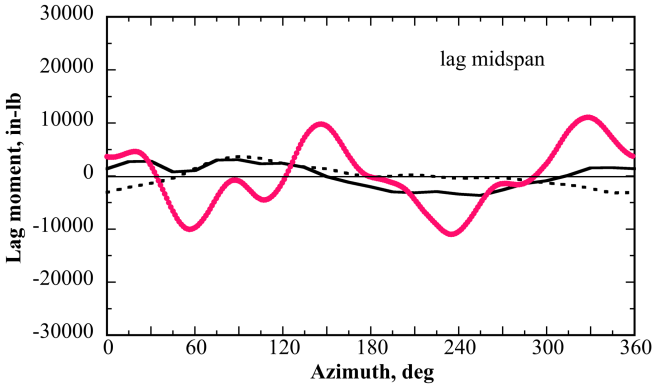

(b) Midspan

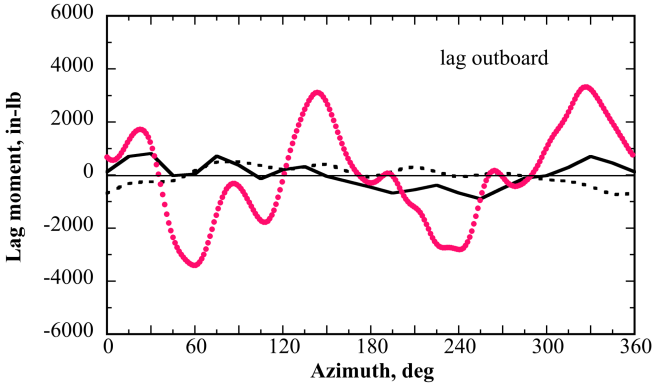

(c) Outboard, scale change

Figure 37. Lag moment time histories, helicopter mode, 75-deg yaw, Ω=573, V=70 knots, μ=0.151, C_T/σ =0.081.

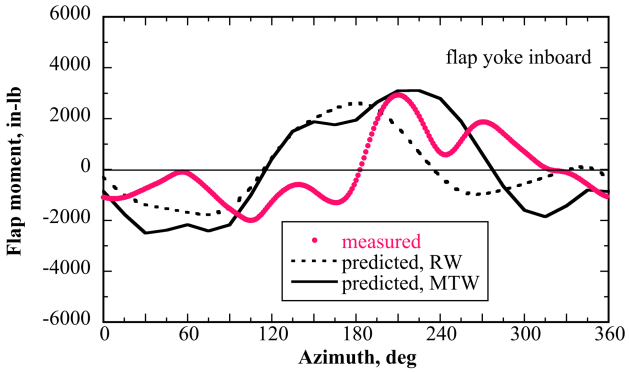

(a) Yoke inboard

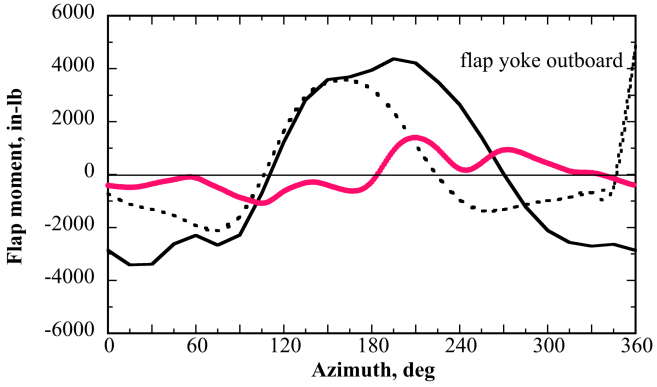

(b) Yoke outboard

Figure 38. Yoke flap moment time histories, helicopter mode, 75-deg yaw, Ω=573, V=70 knots, μ=0.151, C_T/σ =0.081.

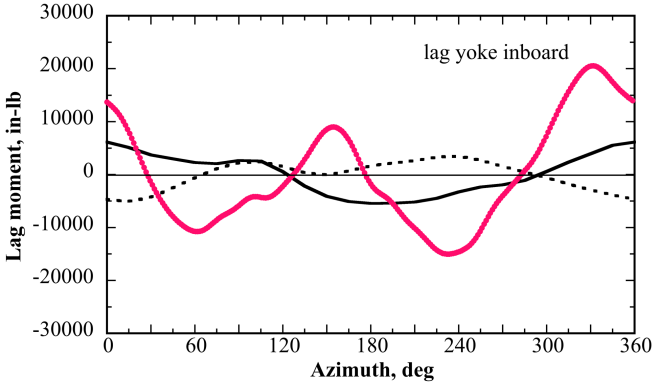

(a) Yoke inboard

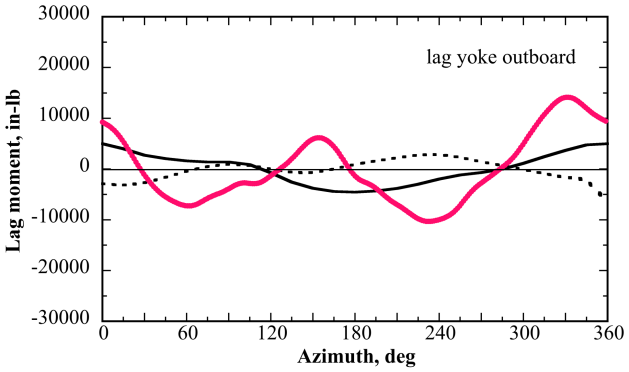

(b) Yoke outboard (lag)

Figure 39. Yoke lag moment time histories, helicopter mode, 75-deg yaw, Ω=573, V=70 knots, μ=0.151, C_T/σ =0.081.

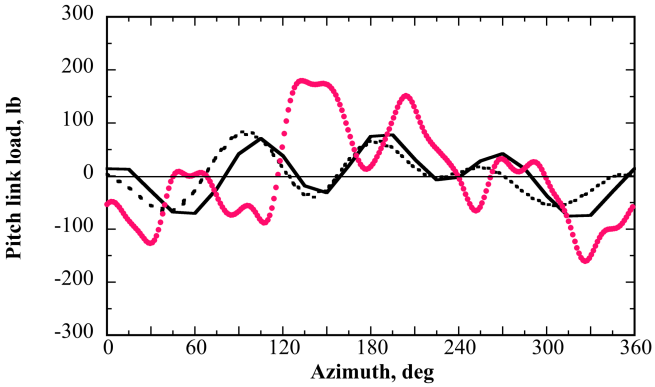

Figure 40. Pitch link load time history, helicopter mode, 75-deg yaw, Ω=573, V=70 knots, μ=0.151, C_T/σ =0.081.

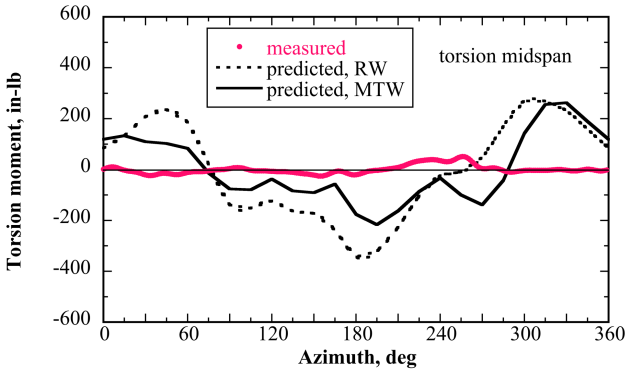

(a) Midspan (torsion)

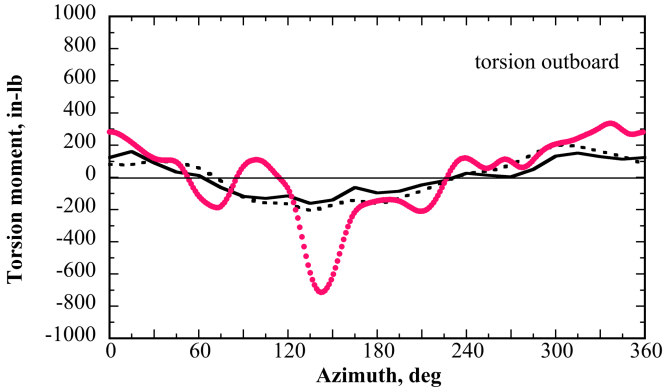

(b) Outboard (torsion)

Figure 41. Torsion moment time histories, helicopter mode, 75-deg yaw, Ω=573, V=70 knots, μ=0.151, C_T/σ =0.081.

To summarize, the ½ peak-to-peak correlations (Figures 29-35) and the time-history correlations (Figures 36-41) show that:

- The MTW multiple-trailer wake model improves the correlation slightly.
- The collective is predicted well by the RW model, the lateral cyclic correlation is not good, and the longitudinal cyclic correlation is reasonable.
- The flap moment correlation is reasonable.
- The lag moment is underpredicted.
- The pitch link load is underpredicted.
- The torsion moment correlation is poor and needs further study.

These are preliminary conclusions, based on only one operational conditional (75-deg yaw, Ω=573, V=70 knots, μ=0.151, and C_T/σ =0.081). Analyzing additional operating conditions should give a more conclusive assessment of the correlation level that can be achieved using a comprehensive analysis. To improve the correlation within the comprehensive analysis framework, one could attempt to fine tune the multiple-trailer wake model (MTW model).

The predictions in this paper are based on a comprehensive analysis and lifting line theory. A completely isolated rotor is modeled. The airflow around the TTR (a relatively large structure, extending over 30 ft in length) is not modeled and as noted earlier, wind tunnel wall effects are not included. It has not yet been determined whether the proximity of the TTR and rotor to the wind tunnel walls has a significant effect or not. A CFD analysis of the complete TTR/699/40x80-test section configuration may resolve this uncertainty. In any case, such considerations are outside the scope of the present study.

CONCLUDING REMARKS

An initial correlation of full-scale 699 proprotor performance and loads for four low-speed conditions was presented in this paper. The conditions included: hover (vertical climb), cruise (airplane), conversion, and helicopter modes. The comprehensive analysis CAMRAD II and recently acquired wind tunnel test data were used. Mean and ½ peak-to-peak quantities (hpp) were correlated; time-history correlation for the helicopter condition was also included.

The hover calculations proved useful in providing reality checks on the test hardware such as: a) the functioning of the installed blade strain gages and b) calibration of the measurement of the collective pitch hardware.

For the cruise and conversion conditions, where the mean and hpp quantities were correlated, reasonable correlation was obtained. The trends (with C_T/σ) were largely captured, with some overprediction or underprediction, elaborated as follows. The thrust correlation was reasonable, with underprediction at low collective. The torque correlation was good to excellent, with the cruise torque slightly underpredicted at high C_T/σ. Both types of discrepancies (thrust and torque) need further study, this could include inclusion of wind tunnel wall effects. The trim cyclic angles correlation was good (conversion). The pitch link load correlation was reasonable, with the trends largely captured. For the flap moment, the trends were captured (except for the yoke moments), there was overprediction or underprediction, and the mean midspan moment correlation was excellent. For the lag moment, the trends were captured, the mean loads were overpredicted, and the hpp correlation was reasonable.

For the helicopter mode, the time-history correlations showed that, compared to the rolled-up wake (RW) model, the multiple-trailer wake (MTW) model improved the correlation slightly. The collective was predicted well by the RW model, the lateral cyclic correlation was not good, and the longitudinal cyclic correlation was reasonable. The flap moment correlation was reasonable. The lag moment and pitch link load were underpredicted. The torsion moment correlation was poor and needs further study. To improve the correlation within the comprehensive analysis framework, one could attempt to fine tune the MTW model.

The current predictions used a comprehensive analysis with lifting line theory, with no wind tunnel wall effects (a completely isolated proprotor was considered). Inclusion of wall effects and the use of higher order airloads from a CFD

analysis may improve the correlation. A full CFD analysis of the TTR/699/40x80-test section configuration may improve the correlation.

Author contact: Sesi Kottapalli *sesi.b.kottapalli@nasa.gov*
C. W. Acree, Jr. *cecil.w.acree@nasa.gov*

ACKNOWLEDGMENTS

Bell Helicopter has been extensively involved with the Tiltrotor Test Rig from inception and also with the 699 research proprotor; the authors gratefully acknowledge the technical support given by Bell Helicopter.

REFERENCES

1. Kottapalli, S. and Acree, C. W., "Analytical Performance, Loads, and Aeroelastic Stability of a Full-Scale Isolated Proprotor," AHS Technical Conference on Aeromechanics Design for Transformative Vertical Flight, San Francisco, California, Jan 16-19, 2018.

2. Kottapalli, S., Russell, C. R., Acree, C. W., and Norman, T. R., "Aeroelastic Stability Analysis of a Full-Scale Isolated Proprotor on the Tiltrotor Test Rig," Dynamics Specialists Conference, AIAA SciTech Forum, San Diego, California, January 7-11, 2019, AIAA-2019-2134.

3. Acree, C. W., Sheikman, A. L., and Norman, T. R., "High-Speed Wind Tunnel Tests of a Full-Scale Proprotor on the Tiltrotor Test Rig," The Vertical Flight Society 75th Annual Forum Proceedings, Philadelphia, Pennsylvania, May 2019.

4. Schatzman, N. L. and Malpica, C., "Acoustic Testing of the Tiltrotor Test Rig in the National Full-Scale Aerodynamics Complex 40- by 80-Foot Wind Tunnel," The Vertical Flight Society 75th Annual Forum Proceedings, Philadelphia, Pennsylvania, May 2019.

5. Acree, C. W. and Sheikman, A. L., "Development and Initial Testing of the Tiltrotor Test Rig," AHS International 74th Annual Forum & Technology Display, Phoenix, Arizona, May 14-17, 2018.

6. Bell Helicopter Company, "Advancement of Proprotor Technology. Task II – Wind-Tunnel Test Results." NASA CR-114363, Bell Report 300-099-004, Sept. 1971.

7. Staruk, W. and Datta, A., "Fundamental Understanding, Prediction, and Validation of Tiltrotor Dynamic Loads in Transition Flight Using RANS/FEA," AIAA SciTech Forum, Grapevine, Texas, January 9-13, 2017, AIAA 2017-0859.

8. Ho, J. C. and Yeo, H., "Comparison of Calculated and Measured Blade Loads of the Tilt Rotor Aeroacoustic Model (TRAM)," The American Helicopter Society 73rd Annual Forum Proceedings, Fort Worth, Texas, May 2017.

9. Acree, C. W., "JVX Proprotor Performance Calculations and Comparisons with Hover and Airplane-Mode Test Data", NASA/TM–2009-215380, April 2009.

10. Johnson, W., "CAMRAD II, Comprehensive Analytical Model of Rotorcraft Aerodynamics and Dynamics," Johnson Aeronautics, Palo Alto, California, 1992-1999.

11. Johnson, W., "Technology Drivers in the Development of CAMRAD II," American Helicopter Society, American Helicopter Society Aeromechanics Specialists Conference, San Francisco, California, January 19-21, 1994.

12. Johnson, W., "A General Free Wake Geometry Calculation for Wings and Rotors," American Helicopter Society 51st Annual Forum Proceedings, Ft. Worth, Texas, May 9-11, 1995.

13. Acree, C. W. Jr., "A CAMRAD II Model of the V-22 Rotor for Whirl-Flutter Analysis," NASA TM 2004-212801, July 2004.

14. Johnson, W., "Airloads and Wake Geometry Calculations for an Isolated Tiltrotor Model in a Wind Tunnel," 27th European Rotorcraft Forum, Moscow, Russia, September 11–14, 2001.